

Dynamic Optimal Countermeasure Selection for Intrusion Response System

Alireza Shameli-Sendi, Habib Louafi, Wenbo He, *Member, IEEE*,
and Mohamed Cheriet, *Senior Member, IEEE*

Abstract—Designing an efficient defense framework is challenging with respect to a network's complexity, widespread sophisticated attacks, attackers' ability, and the diversity of security appliances. The Intrusion Response System (IRS) is intended to respond automatically to incidents by attuning the attack damage and countermeasure costs. The existing approaches inherit some limitations, such as using static countermeasure effectiveness, static countermeasure deployment cost, or neglecting the countermeasures' negative impact on service quality (QoS). These limitations may lead the IRS to select inappropriate countermeasures and deployment locations, which in turn may reduce network performance and disconnect legitimate users. In this paper, we propose a dynamic defense framework that selects an optimal countermeasure against different attack damage costs. To measure the attack damage cost, we propose a novel defense-centric model based on a service dependency graph. To select the optimal countermeasure dynamically, we formulate the problem at hand using a multi-objective optimization concept that maximizes the security benefit, minimizes the negative impact on users and services, and minimizes the security deployment cost with respect to the attack damage cost.

Index Terms—Intrusion, Response system, Attack damage cost, Vulnerabilities surface coverage, Multi-objective optimization.

1 INTRODUCTION

DESIGNING a proper defense framework requires comprehensive understanding of attackers' and defenders' abilities. The Intrusion Detection System (IDS) detects hostile activities or exploits in a network, while the Intrusion Response System (IRS) protects the network by selecting appropriate countermeasures to effectively handle malicious activities (e.g., disabling a daemon or adapting the firewall configuration) [1]. The IRS model comprises four main components: *attack damage cost*, *countermeasure positive effect*, *countermeasure negative impact*, and *countermeasure deployment cost*. The attack damage cost represents the amount of damage to an attack target when the existing security controls are either unavailable or ineffective [2]. The countermeasure positive effect represents how much a countermeasure can protect resources, while the negative impact refers to the impact of a countermeasure on services' availability and users' access. The countermeasure deployment cost refers to the administration cost or complexity of adding a security policy in security appliances. Designing a proper IRS framework inherits some challenges:

- *IRS Components Evaluation*: The attack damage cost should be evaluated accurately; otherwise, the automated IRS may needlessly reduce network performance or wrongly disconnect users from the network. Thus, a trade-off between network performance and network security should be established. The countermeasure positive effect component should consider several factors: 1) actual protection of services at different defense points, 2) already

deployed active countermeasures, and 3) countermeasures success/failure to mitigate attacks. For the countermeasure negative impact, we need to take into account the impact of countermeasures on online users and affected services.

- *IRS Components Combination*: To select an optimal countermeasure at attack time, we need to combine the IRS components. However, those components impact different security attributes and do not use the same measurement unit, which makes the combination not straightforward.
- *IRS Dynamicity*: The static evaluation of IRS components results in several weaknesses: 1) the countermeasures can be predicted by attackers, 2) there is no mechanism for evaluating the effectiveness of deployed countermeasures over time (non-adaptive), or 3) it does not reflect the dynamicity of network status; i.e., added/removed services, vulnerabilities, or online users. Hence, a dynamic IRS is needed. However, each IRS component presents specific challenges. The attack damage cost component should consider the number, frequency, and steps of attacks, which may vary considerably. The countermeasure positive effect component should take into account the effectiveness of deployment over time and improved security state. The countermeasure negative impact component should consider the dynamicity of network status. The countermeasure deployment cost component should consider the state of security appliances. For example, inserting a firewall rule requires an analysis of all the existing rules in a firewall in order to determine the proper order for this rule and to commit the updates [18]. As the number of rules increases, the insertion processing time increases.

In this paper, we propose a framework for selecting and deploying optimal countermeasures to intrusions dynamically. The advantage of such deployment is that countermeasures can be fine-

- A. Shameli-Sendi is with the Faculty of Computer Science and Engineering at Shahid Beheshti University (SBU), G. C., Tehran, Iran. E-mail: a_shameli@sbu.ac.ir
- W. He is with the Department of Computer Science, McGill University, Canada. E-mail: {wenbohe}@cs.mcgill.ca
- H. Louafi and M. Cheriet are with synchronmedia lab, University of Quebec (ETS). E-mail: habib.louafi.1@ens.etsmtl.ca, mohamed.cheriet@etsmtl.ca

Manuscript received Month xx, 2015; revised Month yy, 2016.

tuned according to the context in which the intrusions are detected. In other words, the IRS will take into consideration the resources being targeted by the attack, resources being used by the user, the load of the system, the severity of dependency between services, the history of previous deployments (countermeasure effectiveness), and the current complexity of security defense points. Thus, countermeasures are not predictable since they are not statically determined. Since attack damage and countermeasure costs impact different attributes, we modeled our problem as multi-objective optimization problem. Thus, our framework provides a set of best solutions (different trade-offs) and selects the optimal one based on the severity of attack damage cost. Compared to the previous work, which consider only two objectives, *maximizing the security performance* and *minimizing the security impact on service quality*, in this paper, in addition to these two objective functions, we consider a third objective function, *minimizing the security deployment cost*.

The main contributions of the proposed framework are as follows: 1) To evaluate the attack damage cost, we consider both the current and the potential damage costs using a service dependency graph. The former represents the damage on non-goal services, whereas the latter refers to future damage in relation to goal service (attacker target), 2) We propose a new model to evaluate the countermeasure positive effect dynamically which is based on the vulnerabilities surface coverage and countermeasure goodness. Moreover, this process takes into account the already deployed active countermeasures; thus, it avoids deploying useless countermeasures, 3) We evaluate the countermeasure negative impact on the basis of direct and backward impacts on services and users. These impacts are modeled using a service dependency graph, 4) We evaluate the countermeasure deployment cost by means of incompatibility and administration costs. We present a dynamic model to measure the complexity of deployment cost over time, and 5) In the case of detection of a compromised vulnerability in our attack defense tree, we identify all attack paths to the goal node and then for each path one optimal countermeasure is selected to secure the path. In other words, we stop the ability of the attacker from different attack paths to compromise the target by a combination of optimal countermeasures.

The rest of this paper is organized as follows: Section 2 provides the IRS background. Section 3 presents our problem statement. Section 4 provides a mathematical formulation of our optimization problem. The proposed framework will be discussed in Section 5. Section 6 discusses the various experimental results. Finally, Section 7 makes some concluding remarks.

2 RELATED WORK

In designing a cost-sensitive IRS, several models have been proposed to attune the attack damage and countermeasure costs. As explained, they do not use the same measurement unit [1], [25]. Some models attempt to put these two costs in the same measurement unit by simplifying the problem [4]–[6]. For example, Balepin et al. [6] propose to consider only availability loss of services affected by the intruder and countermeasure. Other models evaluate attack and countermeasure costs without putting them into the same measurement unit (e.g., [10], [20], [22]–[24]). These models define different parameters to calculate costs separately and then use several techniques to compare them. Since our proposed model lies in this category, to continue, we discuss some highly related frameworks.

Chung et al. [10] propose an attack graph model to detect a multi-step attack. When an attack is detected on a node in the attack graph, a countermeasure selection module measures the benefit of all relevant countermeasures on different places from that node to the target by considering all possible paths in the attack graph. The best countermeasure is the one that brings the highest protection and lowest resource cost and intrusiveness to the service level agreement (SLA). This approach suffers from a number of limitations. First, although they state that the problem is a multi-objective optimization one, they reduce it to a single-objective optimization problem, which provides a single solution. They combine the objectives using the well-known ROI (Return of Investment) function, which does not belong to any studied combination methods (known as scalarization [8]). Second, countermeasure cost and intrusiveness on SLA are static values initialized in advance. Therefore, the only objective that varies in function of countermeasures is the benefit objective. That is, their problem, by its nature, is a single-objective optimization problem (maximizing the benefit). Third, they define the effectiveness as the percentage of probability changes of the node, for which the countermeasure is applied, meaning that it is dynamic. However, in the experiments, they use static values. Finally, they do not consider the effectiveness overlap between all the candidate countermeasures and the already deployed active ones.

Granadillo et al. [22] propose a Return on Response Investment (RORI) model to evaluate countermeasures. Several parameters are considered to find the optimal solution: *attack damage*, *countermeasure positive effect*, *countermeasure cost*, and *security equipment cost*. They propose the countermeasure surface coverage to calculate the amount of risk reduction. This approach suffers from several limitations. First, the countermeasure surface coverage is defined as the percentage of attack surface it covers. However, in practice, it is not straightforward to establish a mapping between countermeasures and attacks. Second, in this model, it is possible to apply more than one countermeasure simultaneously. In this case, the surface of one countermeasure may be partially or totally covered by others. Since the countermeasure surface coverage is presented by a percentage, we cannot decide whether or not there is a joint surface. In the case of a possible joint surface, they use the average between the maximum and minimum surface coverage, which is not always reliable from the security perspective. Third, they do not consider the countermeasure's negative impact on services. Sometimes, the maximum benefit brings the maximum impact on service availability. Finally, regarding multi-objective optimization, this model suffers from the same problem as [10] does.

In this paper, we propose a framework that identifies all the best countermeasures and selects the optimal one, without the aforementioned limitations. The proposed framework answers the following questions: 1) how much are the current and potential damage costs when the attack scenarios and attacker's abilities vary, 2) how accurate is the countermeasure risk reduction, 3) how big is the countermeasure impact on QoS, and 4) how can the countermeasure and attack damage costs be efficiently balanced?

3 PROBLEM STATEMENT

Let DS be a defense system deployed on a set of defense points $\mathcal{DP} = \{dp_i\}_{i=1}^n$, each of which is intended to protect a set of services. Let $CM = \{cm_k\}_{k=1}^r$ be a set of possible countermeasures that can be deployed on all the defense points, where r is their

total number. When an attack is detected by the IDS, the attack damage cost is assessed to determine the value of the loss incurred by a compromised service. Then, the optimal countermeasure is identified and deployed to mitigate the attack with respect to the attack severity. Each countermeasure, cm_k , provides three attributes: (1) *Security performance*: it represents the security benefit provided to the defense system when the countermeasure cm_k is activated. We note this property by $\mathcal{S}_P(cm_k)$, (2) *Security impact on service quality*: it represents how much the quality of the services is affected when cm_k is deployed. This can be restricted only to availability, since countermeasures are basically not intended to affect the service's confidentiality or integrity. We denote this property by $\mathcal{S}_Q(cm_k)$, and (3) *Security cost*: it represents the countermeasure deployment cost. It is expressed as the incompatibility (e.g., adding a firewall rule) and administration (e.g., patching a vulnerability) costs. We denote this property by $\mathcal{S}_C(cm_k)$.

The goal is to identify the optimal countermeasure (cm_k^*) that maximizes the security performance, minimizes the security impact, and minimizes the security cost. Therefore, cm_k^* can be computed by solving the following multi-objective optimization problem.

$$\begin{aligned} \text{MOPT } \max & \mathcal{S}_P(cm_k) \\ \min & \mathcal{S}_Q(cm_k) \\ \min & \mathcal{S}_C(cm_k) \\ \text{s.t. } & \mathcal{S}_P(cm_k) \geq s_p, \mathcal{S}_Q(cm_k) \leq s_q, \text{ and } \mathcal{S}_C(cm_k) \leq s_c \end{aligned} \quad (1)$$

where the constraints s_p , s_q , and s_c represent the threshold for the accepted minimum security performance at attack time, accepted maximum security impact on service quality, and accepted maximum cost of countermeasure deployment, respectively. Later in the paper, we will show how these functions can be evaluated.

4 MULTI-OBJECTIVE FORMULATION

In this section, first we formulate our problem with the multi-objective concept and show how to identify the optimal solution. Then, we provide the advantage of multi-objective formulation compared to the existing works in state-of-art.

4.1 Pareto Optimal Set Selection

Let $\Omega \subseteq CM$ be the set of feasible countermeasures that satisfy the constraints of (1). Let $\hat{\Omega}$ be the set of the corresponding triplets $(\mathcal{S}_P(cm_k), \mathcal{S}_Q(cm_k), \mathcal{S}_C(cm_k))$ of Ω in the objective (also called criteria [8]) space. We define \mathcal{H} as a function between Ω and $\hat{\Omega}$ as follows:

$$\begin{aligned} \mathcal{H} : \Omega &\rightarrow \hat{\Omega} \\ cm_k &\mapsto (\mathcal{S}_P(cm_k), \mathcal{S}_Q(cm_k), \mathcal{S}_C(cm_k)) \end{aligned} \quad (2)$$

Let cm_i and cm_j be two feasible countermeasures, and $\mathcal{H}(cm_i)$ and $\mathcal{H}(cm_j)$ their images by \mathcal{H} , respectively, which are given by:

$$\begin{aligned} \mathcal{H}(cm_i) &= (\mathcal{S}_P(cm_i), \mathcal{S}_Q(cm_i), \mathcal{S}_C(cm_i)) \\ \mathcal{H}(cm_j) &= (\mathcal{S}_P(cm_j), \mathcal{S}_Q(cm_j), \mathcal{S}_C(cm_j)) \end{aligned} \quad (3)$$

In the multi-objective optimization, we say that $\mathcal{H}(cm_i)$ dominates $\mathcal{H}(cm_j)$, and we denote it by $\mathcal{H}(cm_i) \succ \mathcal{H}(cm_j)$, if the following inequalities are satisfied:

$$\begin{aligned} &\mathcal{S}_P(cm_i) > \mathcal{S}_P(cm_j) \wedge \mathcal{S}_Q(cm_i) \leq \mathcal{S}_Q(cm_j) \wedge \mathcal{S}_C(cm_i) \leq \mathcal{S}_C(cm_j) \\ &\text{or} \\ &\mathcal{S}_P(cm_i) \geq \mathcal{S}_P(cm_j) \wedge \mathcal{S}_Q(cm_i) < \mathcal{S}_Q(cm_j) \wedge \mathcal{S}_C(cm_i) \leq \mathcal{S}_C(cm_j) \\ &\text{or} \\ &\mathcal{S}_P(cm_i) \geq \mathcal{S}_P(cm_j) \wedge \mathcal{S}_Q(cm_i) \leq \mathcal{S}_Q(cm_j) \wedge \mathcal{S}_C(cm_i) < \mathcal{S}_C(cm_j) \end{aligned} \quad (4)$$

Clearly, solution cm_i is better than solution cm_j , that is, cm_i provides security performance higher than or equal to cm_j with lower or equal impact on service quality, and lower or equal security cost. However, there are many solutions that provide different trade-offs between security performance, security impact on service quality, and security cost. In this sub-space of solutions, any improvement in one objective function is automatically compensated by a deterioration in one or more of the other objectives. Therefore, to solve (1), we evaluate all the solutions that cannot be dominated by any other solution, from which we identify the optimal one. Such solutions are called *Pareto optimal solutions* and their images in the objective space are called *Pareto optimal set*. Let $\Omega_p \subseteq \Omega$ and $\hat{\Omega}_p \subseteq \hat{\Omega}$ be, respectively, the Pareto optimal solution space and the Pareto optimal set (its image by \mathcal{H}). This Pareto optimal solution space is given by:

$$\forall cm_i \in \Omega_p, \nexists cm_j \in \Omega \mid \mathcal{H}(cm_j) \succ \mathcal{H}(cm_i) \quad (5)$$

4.2 Optimal Solution Selection

Several methods can be used to extract the optimal solution from the Pareto optimal set [8], [11]. In this paper, SAW is used since it provides reasonable result (see section 6.6.1). The SAW method consists in weighting all the objective functions and summing them up. It comprises two steps: normalization of the objective functions and evaluation of the final score of each countermeasure. For each countermeasure $cm_k \in \Omega_p$, the normalization is as follows:

$$\begin{aligned} \tilde{\mathcal{S}}_P(cm_k) &= \frac{\mathcal{S}_P(cm_k)}{\max_{cm_i \in \Omega_p} (\mathcal{S}_P(cm_i))} \\ \tilde{\mathcal{S}}_Q(cm_k) &= \frac{\min_{cm_i \in \Omega_p} (\mathcal{S}_Q(cm_i))}{\mathcal{S}_Q(cm_k)} \\ \tilde{\mathcal{S}}_C(cm_k) &= \frac{\min_{cm_i \in \Omega_p} (\mathcal{S}_C(cm_i))}{\mathcal{S}_C(cm_k)} \end{aligned} \quad (6)$$

where $\tilde{\mathcal{S}}_P$, $\tilde{\mathcal{S}}_Q$, and $\tilde{\mathcal{S}}_C$ are the normalized values of \mathcal{S}_P , \mathcal{S}_Q , and \mathcal{S}_C , respectively. Note that this is not the unique way of normalization [11].

The final score of each countermeasure cm_k , which we denote by $\mathcal{Q}(cm_k)$, is evaluated as follows:

$$\mathcal{Q}(cm_k) = w_P \cdot \tilde{\mathcal{S}}_P(cm_k) + w_Q \cdot \tilde{\mathcal{S}}_Q(cm_k) + w_C \cdot \tilde{\mathcal{S}}_C(cm_k) \quad (7)$$

where w_P , w_Q , and w_C are weights used to favor one objective over the others in order to select the optimal security countermeasure from the Pareto optimal set. In general, to express the relative importance between the objective functions and not to use large values, these weights should satisfy the following properties:

$$\begin{aligned} w_P + w_Q + w_C &= 1 \\ w_P > 0, w_Q > 0, w_C > 0 \end{aligned} \quad (8)$$

When the attack damage cost is high, a strong countermeasure should be selected, and vice versa. This means that damage cost is aligned with the security performance. Therefore, we propose to set the value of w_P as the attack damage cost. For example, if the damage cost is 90%, the sum of two other weights is 10% (w_Q and w_C). Thus, the second and third objectives are less important. To decide about the relative importance between the second and third objectives, we introduce σ and θ . If the services provided by the company are more important than the cost of deploying a countermeasure, a higher value of σ should be set, and vice versa. Thus, we have:

$$\begin{aligned} w_P &= \text{attack damage cost} \\ w_Q &= (1 - w_P) \cdot \sigma / (\sigma + \theta) \\ w_C &= (1 - w_P) \cdot \theta / (\sigma + \theta) \\ \sigma + \theta &= 1, \sigma > 0, \theta > 0 \end{aligned} \quad (9)$$

The optimal countermeasure, cm_k^* , is the one that yields the highest Q value. It is given by:

$$cm_k^* = \arg \max_{cm_k \in \Omega_P} Q(cm_k) \quad (10)$$

4.3 Advantages

As explained earlier, first we identify all the best possible solutions, those lying on the Pareto optimal set. Then, from the latter, we extract the optimal one using the SAW method. This way, we ensure that the obtained solution belongs to the Pareto optimal set. In contrast, other works [10], [22] combine the objective functions without evaluating the Pareto optimal set. They reduce the multi-objective problem into a single objective optimization one, and select the optimal solution from the combined solution space. The question is when to convert the problem into a single objective optimization one (e.g., SAW): 1) from the beginning, on all the solution space or 2) on the Pareto optimal solution space. According to research performed in multi-objective optimization, the methods that consist in combining the objective functions without evaluating the Pareto optimal set, from the beginning, do not guarantee a non-dominated solution [8].

5 PROPOSED FRAMEWORK

Figure 1 illustrates the proposed architecture of our automated intrusion response system. There are two data structures in our model: *Attack-Defense Trees (ADT)* and *Service Dependency Graph (SDG)*. In a large network model, different ADTs can be defined based on the SDG in such a way that each ADT protects one goal service. Note that our framework works with one ADT, which is selected by the security expert. Over time, we may select another ADT, following the new strategy of the company. When an alert is raised by IDS, our framework maps the alert to the selected ADT, from which all possible attack paths to the target are extracted. Then all defense points are identified for each attack path. On the basis of the type of defense point, appropriate countermeasures are selected. Next, for all of them three functions are evaluated independently: the *security benefit*, *security impact*, and *security cost*. A Pareto optimal set is generated to see which countermeasures satisfy the trade-off between these three functions. Finally, the optimal countermeasure is selected from the Pareto optimal set with respect to the severity of the attack. The latter is measured by the attack damage cost component which is based on the SDG. Once the optimal countermeasure

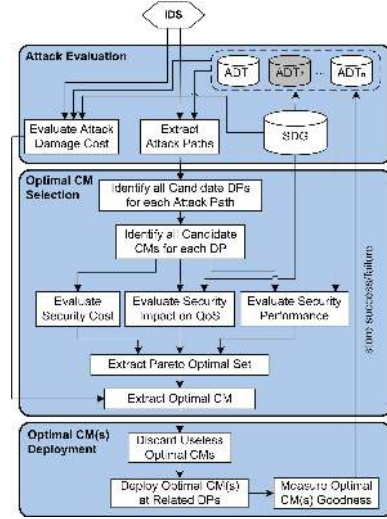


Fig. 1: Proposed architecture.

of each attack path is identified, the useless ones (those whose effect is covered by another) are eliminated. Then, the remaining countermeasures are deployed and their effectiveness at the related defense points is measured and stored in the relevant ADT. To continue, we first explain the SDG and ADT data structures, then detail the main components of our IRS as illustrated in Figure 1.

5.1 Service Dependency Graph

We say that a service s_i depends on another service s_j if s_i needs s_j to function properly. For instance, in the case of dependency between a web server and a database, if the web server is to function properly, the database must be available and its data not be corrupted. Conversely, if the database is not available (e.g., it is down) or its data are altered, the web server will either not provide information or provide the wrong information. We call this, functional dependency between services.

However, the attacker may exploit non-functional connections to reach his target. Let machines M1 and M2 host Apache and DB, respectively. Suppose that sshd, running on M2, does not need to communicate with any service. The attacker first compromises Apache and obtains root access on M1. Then, he uses the connection between M1 and M2 to compromise sshd's vulnerability and become rooted in M2. Finally, he becomes able to compromise DB without using the connection between Apache and DB. We call this, non-functional dependency between services.

In this paper, we model these types of dependencies by means of a service dependency graph (SDG), the vertices being the services, and the edges being the functional and non-functional dependencies between them. To each vertex s_k in the graph, we associate a vector $I(s_k)$ which represents the importance of the service (also called service value), in terms of CIA (confidentiality, integrity, and availability). Besides, to each edge between s_i and s_k in the graph (s_i depends on s_k), we associate a vector that consists of three weight values that represent the dependency severity $d_{i,k}^{\{C,I,A\}} \in [0, 1]$ in terms of CIA. Note that for the non-functional dependency, the CIA values are set to zero. The severity models how strong the dependency between s_i and s_k is, which reveals how much the damage incurred on s_k will affect s_i . For instance, in a denial of service (DoS) attack on s_k , the attacker slows down the functionality of s_k . This decreases the service availability (A) of s_k , and does so on all the services that depend

on s_k . In the User to Root (U2R) or Remote to Local (R2L) attack types, since s_k is under the control of the attacker, all CIA parameters of s_k and those of the services that depend on it can be affected. Both the importance of services and the dependency severity between them are defined by the security expert. As seen in Figure 1, SDG is used in measuring the attack damage cost and security impact on QoS.

5.2 Attack-Defense Tree

To understand the attacker’s progress and find the attack path to the attacker’s target, there are two approaches to model network vulnerabilities: an attack graph [12], [13] and an attack tree [14], [15]. They provide an appropriate picture of different ways for compromising a target by exploiting a sequence of vulnerabilities. The attack tree tackles the state space explosion problem, which is present in the graph, and consequently addresses the problem of visualization complexity [16]. In this paper, we use the *Attack-Defense Tree* which consists of two types of actions: *attacker action* and *defender action*. We define our ADT as follows:

Definition 1 (Attack-Defense Tree (ADT)). *The proposed attack-defense tree is a 4-tuple $ADT = \langle s_g, S_{ng}, V, DP \rangle$, where:*

- 1) s_g is the root of the ADT, which represents the attacker-targeted service (goal service).
- 2) $S_{ng} = \{s_i\}_{i=1}^d - \{s_g\}$ represents the set of services that are compromised (non-goal services) to reach the attacker’s target.
- 3) $V = \bigcup_{i=1}^d V(s_i)$ is the set of vulnerabilities that are present in the network topology. For a given service s_i , let $V(s_i) = \{v_j(s_i)\}_{j=1}^m$ be the set of its vulnerabilities. To compromise s_i through functional dependency, the predicate $\bigvee_k \left(\bigwedge_t v_t(s_i) \right)$ should be true. k represents the number of disjunctions and t refers to the number of conjunctions in each disjunction. That is, at least one term of this disjunction should be true. In non-functional dependency, a service may be compromised without exploiting any vulnerability. For more details and examples, the reader is referred to [17].
- 4) $DP = \{dp_i\}_{i=1}^n$ is a set of defense nodes placed in the ADT to protect services. Thus, each node, s_i , may have one child, representing at least a defense point. For each defense point, we assign a list of appropriate countermeasures. Some of them are general countermeasures (e.g., restarting a service/machine) though others are defined with respect to the type of service.

In a multi-step attack, the attacker compromises a set of services (non-goal) to reach his target. To do so, he has to exploit one or more of the vulnerabilities of a non-goal service in each step. Figure 2 represents a general ADT. Two types of sub-graphs are presented in the figure: *star* and *diamond*. The star sub-graph includes at least one vulnerability that results in full access to the root of that sub-graph. In the diamond sub-graph, there is no vulnerability that leads to full-access to the root of the sub-graph (limited access to root). Thus, depending on the attack type impact on the root of the sub-graph, the attacker has different opportunities to reach the next level (see (15)). If the attacker comes from the star sub-graph, he is able to compromise all the vulnerabilities of the next level. Otherwise, he has limited access and may compromise only a set of them.

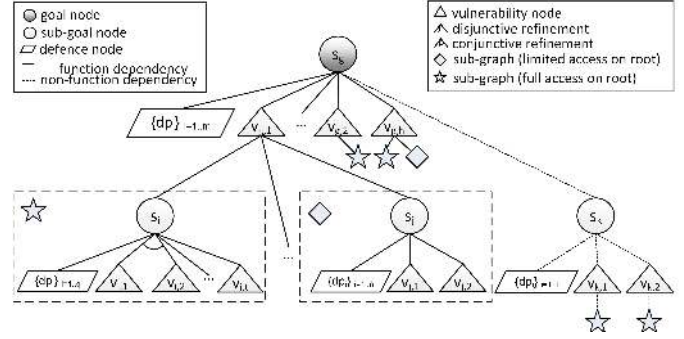


Fig. 2: General Attack-Defense Tree.

The ADT is created first and then updated over time, when services or vulnerabilities are added/removed. In case of updating the ADT during attack time, the update cost does not impact the optimal countermeasure selection process, since it uses the current (not being updated) ADT. That is, the attack is based on the current ADT version, as the updated one has not known to the attacker yet.

There are four cases to update ADT. (1) If a new vulnerability v_x is discovered for a given service s_x , all the services that depend on s_x are identified (using SDG). If v_x needs limited access permission to be compromised, all the identified services are connected. Otherwise, only the services that can be compromised as full access are connected. (2) In case of removing a vulnerability, protected by a countermeasure, the ADT is updated by removing the sub-graph, the root of which is v_x . This keeps the ADT optimized, by eliminating useless attack paths (see Section 5.4). (3) If a new service is added, a new sub-graph, the root of which is that service and the children are its vulnerabilities, is created. If the root can be compromised as full access, it is connected to all the vulnerabilities of the services it uses. If there is no vulnerability that leads to full-access to root of sub-graph (limited access to root), the root is connected to the vulnerabilities, which need limited access permission to be compromised. Then, each child is connected to the ADT following the same process of connecting a new vulnerability. (4) Similar to vulnerability, removing a service consists in eliminating the sub-graph rooted by that service.

5.3 Attack Damage Cost Evaluation

Attackers are smart people in reality and they know that they may not achieve their malicious goals if they just follow the standard steps to compromise the target. They try to find the vulnerable services and defense points of the network and bypass them (non-goal services) to launch multi-step attacks and compromise the target (goal service). Two techniques can be used to calculate the attack damage cost in this context [7]: *attack-centric* and *defense-centric*. In attack-centric, there is one goal (e.g., a sensitive file modification) and all other completed steps are called non-goal. In this model, if the attacker does not reach the target goal, the attack damage cost is zero. However, the defender may not know the attack type and the attacker’s real intention until the end of an accomplished multi-step attack. Therefore, we should consider the uncertainty about the attackers’ activities in the selection of the best countermeasure. Thus, we propose a defense-centric model to take into account not only the current damage but also the potential damage of the multi-step attack. The current damage is the damage incurred on compromised services (non-goal) and the potential damage represents the attack damage in the next step of attack (non-goal/target). Thus, our model not only protects against

any attack on goal-service (e.g., compromising Database) but also any attack on non-goal services (e.g., DDoS on Web service). We evaluate these two damages using the service dependency graph (defined in Section 5.1). Thus, the total attack damage cost for the whole system (S) from the exploited vulnerability v_j in service s_k is the ratio of the importance of the services damaged by attacker to the total importance of all services in terms of CIA. This cost is calculated as follows:

$$D(S, s_k, v_j) = \frac{\sum_{\delta \in \{C, I, A\}} D_\delta(S, s_k, v_j)}{\sum_{s_i \in S} \sum_{\delta \in \{C, I, A\}} I_\delta(s_i)} \quad (11)$$

where $D_C(S, s_k, v_j)$, $D_I(S, s_k, v_j)$, and $D_A(S, s_k, v_j)$ are attack damage cost in terms of confidentiality, integrity, and availability, respectively. $I_C(s_i)$, $I_I(s_i)$, and $I_A(s_i)$ represent the importance of the service s_i in terms of confidentiality, integrity, and availability, respectively. The attack damage cost for each attribute (C, I, A) is evaluated as follows:

$$D_\delta(S, s_k, v_j) = D_\delta^c(S, s_k, v_j) + D_\delta^p(S, s_k, v_j) \quad (12)$$

where $D_\delta^c(S, s_k, v_j)$ and $D_\delta^p(S, s_k, v_j)$ are the current and potential attack damage costs, respectively. To calculate the current damage cost, direct and backward propagation are considered. In the backward sub-graph of service s_k , $B(s_k)$, the damage propagation is considered for all services that have mandatory dependency on s_k directly or indirectly. In mandatory dependency, a service requires the functionality of one or many service(s) on which it directly or indirectly depends on. Thus, the current damage cost is calculated as follows:

$$D_\delta^c(S, s_k, v_j) = \overline{D}_\delta^c(S, s_k, v_j) + \overleftarrow{D}_\delta^c(S, s_k, v_j) \quad (13)$$

where $\overline{D}_\delta^c(S, s_k, v_j)$ and $\overleftarrow{D}_\delta^c(S, s_k, v_j)$ are the direct and backward propagated attack damages, respectively. They are given by:

$$\begin{aligned} \overline{D}_\delta^c(S, s_k, v_j) &= A_m^c(s_k, A_t^c(v_j))I(s_k) \\ \overleftarrow{D}_\delta^c(S, s_k, v_j) &= \sum_{s_i \in B(s_k)} A_m^{bc}(s_{i+1} : s_i) d_{i,i+1} I(s_i) \end{aligned} \quad (14)$$

where $A_m^c(s_k, A_t^c(v_j))$ is the attack impact on s_k , which depends on the type of attack (A_t^c), when vulnerability v_j is exploited (as seen in (15)).

$$A_m^c(s_k, A_t^c(v_j)) = \begin{cases} [1, 0, 0] & \text{if } A_t^c(v_j) = \text{information leakage} \\ [1, 1, 1] & \text{if } A_t^c(v_j) = \text{remote-2-root} \\ [0, 1, 0] & \text{if } A_t^c(v_j) = \text{integrity} \\ [0, 0, 1] & \text{if } A_t^c(v_j) = \text{denial-of-service} \\ \dots & \dots \end{cases} \quad (15)$$

$A_m^{bc}(s_{i+1} : s_i)$ is the backward attack impact propagation from s_{i+1} to s_i . It is calculated as follows:

$$A_m^{bc}(s_{i+1} : s_i) = \begin{cases} A_m^c(s_{i+1}, A_t^c(v_j)) & \text{if } s_{i+1} = s_k \\ A_m^{bc}(s_{i+1}) d_{i+1, i+2} & \text{else} \end{cases} \quad (16)$$

Since the attack starts from s_k , the impact on all the parents of s_k (in service dependency graph) is equal to the impact on s_k , $A_m^c(s_k, A_t^c(v_j))$. For other services (e.g., s_i), which depend to the

parents of s_k , the backward attack impact propagation depends on the type of attack impact on the service s_{i+1} and CIA dependency vector between s_{i+1} and s_{i+2} . The attack impact on CIA in s_k cannot be propagated to all services in the backward sub-graph. At each step of the evaluation, the impact propagation value should be moderated on the basis of the CIA dependency between services.

To perform the potential damage cost evaluation, we follow the forward dependency direction from service s_k , $F(s_k)$, to identify all the services that can be affected in the next step of the multi-step attack. The potential damage cost is calculated as follows:

$$D_\delta^p(S, s_k, v_j) = \sum_{s_i \in F(s_k)} \overline{D}_\delta^p(S, s_i, v_h^*) + \overleftarrow{D}_\delta^p(S, s_i, v_h^*) \quad (17)$$

where $\overline{D}_\delta^p(S, s_i, v_h^*)$ and $\overleftarrow{D}_\delta^p(S, s_i, v_h^*)$ are the potential attack damages on service s_i , which is exactly one step ahead from the compromised service (s_k), and the backward propagated attack damage from it, respectively. Since the attacker's intention cannot be known in advance, it is useless to evaluate the potential attack damage for all steps ahead from s_k . Thus, we gradually evaluate the attack damage on the basis of the attacker's behavior. The direct and potential damages are given by:

$$\begin{aligned} \overline{D}_\delta^p(S, s_i, v_h^*) &= A_m^p(s_i, A_t^p(v_h^*))I(s_i) \\ \overleftarrow{D}_\delta^p(S, s_i, v_h^*) &= \sum_{s_j \in B(s_i) - \{s_k\}} A_m^{bp}(A_m^p(s_{j+1} : s_j)) d_{j, j+1} I(s_j) \end{aligned} \quad (18)$$

where $A_m^p(s_i, A_t^p(v_h^*))$ is the attack impact on s_i when v_h^* is exploited. v_h^* is the vulnerability that creates the highest damage on s_i once it is exploited. It is given by:

$$v_h^* = \arg \max_{v_h \in V(s_i)} A_t^p(v_h) \quad (19)$$

$A_m^{bp}(A_m^p(s_{j+1} : s_j))$ is the backward impact propagation from s_{j+1} to s_j calculated using the same formula expressed in (16).

5.4 Attack Paths Extraction

Once an attacker compromises a vulnerability, he may use different attack paths to compromise the target. Thus, when an IDS generates an alert about a compromised vulnerability, all attack paths are extracted and secured. In other words, our model stops the ability of the attacker to use different attack paths to compromise the attacker's target when a vulnerability is compromised. Note that in the attack paths extraction, we eliminate the redundant attack paths, which visit the same sequence of defense points. This is common in an attack tree, since the goal/non-goal node(s) may have more than one vulnerability (see the star shape in Figure 2).

As shown in Figure 2, the extracted attack paths are injected into an "Optimal CM selection" engine, where for each attack path, all defense points are identified and used in selecting the optimal countermeasure. In the next subsections, we will explain how security performance, security impact on QoS, and security cost are evaluated for each candidate countermeasure.

5.5 Objective Functions Evaluation

5.5.1 Security Performance Evaluation

Our security performance evaluation is based on the countermeasure positive effect, which takes into account two features: *vulnerabilities surface coverage* and *goodness* (or *effectiveness*).

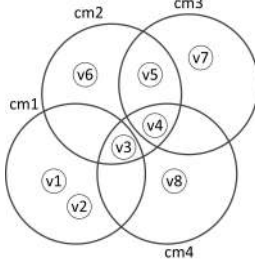


Fig. 3: Example of CMs vulnerabilities surface coverage.

Definition 1: The vulnerabilities surface coverage (VSC) of a countermeasure cm_k is the number of vulnerabilities it covers. It is of two kinds: disjoint and joint. The former includes the vulnerabilities covered only by cm_k , whereas the latter refers to the vulnerabilities covered by cm_k and others.

Note that some countermeasures, which do not affect the services or whose impact is not permanent, are not considered in the VSC model. For example, blocking the attacker IP address, restarting a virtual machine (VM), closing a connection, and all initial firewall rules (set up by the administrator). Figure 3 shows the concept of vulnerabilities surface coverage of four countermeasures deployed on a given defense point. Suppose that these four countermeasures are applied at different times in this order: cm_1 , cm_2 , cm_3 , then cm_4 . When cm_2 is applied after cm_1 , it covers not only vulnerabilities v_4 , v_5 , and v_6 but also vulnerability v_3 that has been already covered by cm_1 . To understand how much our security will be improved by applying cm_2 , we need to clarify the joint surface. We compare the goodness of cm_1 and cm_2 . If the goodness of cm_2 is bigger than cm_1 , cm_2 should be responsible for the joint surface (v_3). To calculate the total security performance, we remove the joint surface coverage that belongs to cm_1 and add cm_2 's joint surface. Let us consider applying the last countermeasure (cm_4), the goodness of which is bigger than all applied countermeasures. Note that cm_2 and cm_3 are responsible for v_3 and v_4 , respectively. In this case, we remove the joint surface between cm_2 and cm_4 (for v_3), and the joint surface between cm_3 and cm_4 (for v_4). Then, we assign the new joint surface (v_3 and v_4) to cm_4 .

In order to evaluate the goodness of a countermeasure, the majority of the proposed solutions are attack-driven [22]. However, with attack-driven models, it is not straightforward to calculate the attack probability and severity after countermeasure deployment. Moreover, the number of attack types and their severities vary drastically. In this paper, a countermeasure-driven technique is proposed, in which the effectiveness of a countermeasure is measured based on its history (success and failure over time) only.

Definition 2: The goodness of a countermeasure represents the history of its success and failure to mitigate attacks over time. It varies from one defense point $G(dp_i, cm_k)$ to another $G(dp_j, cm_k)$ in ADT.

The evaluation of success and failure of a countermeasure applied on a defense point is based on two factors: 1) efficiency time (Δt); and 2) the progress of any new attempt by attackers within Δt in ADT. When a countermeasure is deployed, we wait for a certain time (Δt), and we check for any attack detection results in any node of ADT. If IDS does not report any alert in Δt duration, it means that the optimal selected countermeasure has succeeded in repelling the attack progress and its success factor is increased by 1; otherwise, its failure factor is increased.

In case of attack, we should calculate the goodness of all countermeasures based on the history of their deployments (success or failure). Since the most recent results must be considered more valuable than earlier ones, we use the aging algorithm by dividing the history into different windows (e.g., day, week, month) confined between 0 and 2. The value of zero represents the worst case when all the history consists of only failures, while the value of two indicates the best case, i.e., only successes. To compute the total goodness of a countermeasure, we propose the following formula:

$$G(dp_i, cm_k) = \sum_{w=1}^n \frac{G_w(dp_i, cm_k)}{2^{(w-1)}} \quad (20)$$

where $G_w(dp_i, cm_k)$ is the goodness of cm_k computed for window w on defense point dp_i , which is presented as follows:

$$G_w(dp_i, cm_k) = \frac{s(dp_i, cm_k)}{s(dp_i, cm_k) + f(dp_i, cm_k)} \quad (21)$$

where s and f are the number of successes and failures evaluated in window w . If there is no history for a given countermeasure in a window, we ignore that window in evaluation. The initial value of success and failure of all countermeasures at starting time (first window) are set to 1 and 0, respectively. In this case, the goodness is equal to 1, which represents a middle goodness value. This value can be updated according to the effectiveness of countermeasures to mitigate attacks over time.

Now, using the countermeasure vulnerabilities surface coverage and goodness features, we show how to evaluate the security performance of countermeasure deployment. Let cm_k be a countermeasure to be deployed on defense point dp_i , where a set of countermeasures CM_a are still active. The actual security performance S_P , after activating cm_k is given by:

$$S_P(dp_i, cm_k) = f_{\bar{s}}(cm_k) + \sum_{cm_i \in CM_a} f_s(cm_i, cm_k) \quad (22)$$

where $f_{\bar{s}}(cm_k)$ and $f_s(cm_i, cm_k)$ are two functions that compute the security performance of cm_k for the disjoint surface and joint surface(s), respectively. They are given by:

$$f_{\bar{s}}(cm_k) = |V_l| \cdot G(dp_i, cm_k) \quad (23)$$

$$f_s(cm_i, cm_k) = \begin{cases} |V_{k,i}| \cdot (G(dp_i, cm_k) - G(dp_i, cm_i)) & \text{if } G(dp_i, cm_k) > G(dp_i, cm_i) \\ 0 & \text{if } G(dp_i, cm_k) \leq G(dp_i, cm_i) \end{cases} \quad (24)$$

where, $G(dp_i, cm_k)$ and $G(dp_i, cm_i)$ are the goodness of cm_k and cm_i , respectively. Let V_k and V_i be the set of vulnerabilities covered by cm_k and cm_i , respectively. $V_{k,i} = V_k \cap V_i$ is a set of vulnerabilities that belong to the joint surface of cm_k and cm_i . $V_l = V_k - (V_k \cap V_i)$ is a set of vulnerabilities that belong to the disjoint surface of cm_k . $|V_{k,i}|$ and $|V_l|$ are the cardinalities of $V_{k,i}$ and V_l , respectively.

5.5.2 Security Impact on Service Quality Evaluation

To evaluate the impact of the countermeasure deployment on service quality, we use the directed service dependency graph (SDG) (defined in Section 5.1). In such a graph, for each service s_j , we have two sub-graphs: *forward* and *backward*. The former comprises the set of services on which s_j depends, and the latter comprises the set of services that depend on s_j . Using that

dependency graph, the impact of activating a countermeasure cm_k on service quality on the defense point dp_i is given by:

$$\mathcal{S}_Q(dp_i, cm_k) = \overline{\mathcal{S}}_Q(X_i^k, cm_k) + \overleftarrow{\mathcal{S}}_Q(X_i^k, cm_k) + \overrightarrow{\mathcal{S}}_Q(X_i^k, cm_k) \quad (25)$$

where X_i^k represents the set of services affected by cm_k from those covered by the defense point dp_i . $\overline{\mathcal{S}}_Q$ is the impact on service quality for the directly affected services (X_i^k). $\overleftarrow{\mathcal{S}}_Q$ and $\overrightarrow{\mathcal{S}}_Q$ are the impact on service quality for the backward ($B(s_j)$) and forward ($F(s_j)$) sub-graphs of each service $s_j \in X_i^k$, respectively (see Section 5.3). We evaluate them as follows:

$$\begin{aligned} \overline{\mathcal{S}}_Q(X_i^k, cm_k) &= C_p(cm_k)C_t(cm_k) \sum_{s_j \in X_i^k} (U(s_j))^\alpha (I(s_j))^\beta \\ \overleftarrow{\mathcal{S}}_Q(X_i^k, cm_k) &= \\ C_p(cm_k)C_t(cm_k) &\sum_{s_j \in X_i^k} \sum_{\substack{s_l \in B(s_j) \\ \wedge s_l \notin X_i^k}} d_{l,l+1} (U(s_l))^\alpha (I(s_l))^\beta \\ \overrightarrow{\mathcal{S}}_Q(X_i^k, cm_k) &= 0 \end{aligned} \quad (26)$$

where $U(s_l)$, $I(s_l)$, and $d_{l,l+1}$ are, respectively, the number of users of s_l , its importance, and its dependency severity with its child s_{l+1} . For those services that are not directly accessible by users (e.g., DB service), only the administrator is considered the direct user. The values of α and β express the relative importance between the service and the number of users using it from the point of view of the company. Therefore, to express the relative importance between them, we have $\alpha + \beta = 1$. $C_p(cm_k)$ and $C_t(cm_k)$ are the power and type of cm_k to stop attack. Since countermeasures impact only on service availability, we assume:

$$C_t(cm_k) = [0 \ 0 \ 1]^T \quad (27)$$

The countermeasure can be deployed either on a service (e.g., restarting a web service) or on a defense point (e.g., a firewall rule). In both cases, one or more service(s) may be affected. Thus, the backward impact propagation of a countermeasure is defined as the impact on all the services that have a mandatory dependency on the affected service(s), directly or indirectly. It is clear that there is no forward impact propagation.

5.5.3 Security Cost Evaluation

We propose to evaluate the security cost by two criteria, incompatibility cost (IN_C) and administration cost (AD_C). IN_C refers to rule insertion in a firewall while AD_C expresses the human intervention after a countermeasure deployment. Thus, we define these two criteria as follows:

Definition 3: *The incompatibility cost represents the complexity of adding a security policy in security appliances (e.g., adding a rule in firewall).*

Definition 4: *The administration cost represents the time required to return the affected configurations, caused by deployed countermeasures, to the previous states.*

Note that AD_C can be broken down into *installation cost* and *operation cost*. For example, disconnecting a machine incurs operation cost, whereas patching a vulnerability causes installation

cost. However, we group them as one element, namely, administration cost. Thus, we have:

$$\mathcal{S}_C(dp_i, cm_k) = IN_C(dp_i, cm_k)^\gamma \cdot AD_C(cm_k)^\delta \quad (28)$$

where the values of γ and δ express the relative importance between the incompatibility and administration costs, respectively.

Now, we formulate the incompatibility cost of rule insertion in firewall. To avoid creating anomalies in the firewall, inserting a rule requires an analysis of all the existing rules in order to determine its proper order, and committing the updates [18]. As the number of rules increases, the insertion processing time increases. We modeled the incompatibility cost of rule insertion by a modified Smf¹, sigmoidal membership function, in range [1,3]. The original Smf function was in range [0,1]. We modified it for two reasons: 1) because of the product operation in (28), an incompatibility cost value of zero reduces the product to zero, which is not reasonable. That is, if there is no incompatibility cost, the security cost should depend on the administration cost. Therefore, we need to change the range to exclude the zero value; and 2) since the administration cost is in range [1,3], we modified the incompatibility cost range to bring the two functions within the same range. The incompatibility cost function is evaluated as follows:

$$IN_C(dp_i, cm_k) = \text{Smf} \left(r(dp_i), a, b \right) \quad (29)$$

with:

$$\text{Smf} \left(x, a, b \right) = \begin{cases} 1 & \text{if } x \leq a \\ 1 + 4 \left(\frac{x-a}{b-a} \right)^2 & \text{if } a \leq x \leq \frac{a+b}{2} \\ 3 - 4 \left(\frac{x-b}{b-a} \right)^2 & \text{if } \frac{a+b}{2} \leq x \leq b \\ 3 & \text{if } x \geq b \end{cases}$$

where $r(dp_i)$ represents the number of firewall rules on defense point dp_i . The value of a expresses the number of rules that do not create any incompatibility cost ($IN_C = 1$). Incompatibility cost is saturated when the total rules reach the boundary b ($IN_C = 3$). These values can be determined by experience or defined by the security expert [18].

When the countermeasure is not a firewall rule, such as a patch, the incompatibility cost value is 1 (the lowest value, since adding a patch has no impact on incompatibility).

The administration cost can be any score between 1 and 3. In our model, the administration cost of a patch has the highest value. Restarting a firewall or shutting down/restarting a machine has a medium value cost. Those that do not need the administrator's intervention (e.g., adding a rule in firewall) have the lowest value.

5.6 Pareto Optimal Set and Optimal CM Extraction

In previous sections, we explained how to evaluate the security performance, security impact on QoS, security cost, and attack damage cost. Now, we can solve equation (1), by evaluating the Pareto optimal set, from which we extract the optimal countermeasure, as explained in Section 4.

1. <http://www.mathworks.com/help/fuzzy/smf.html>

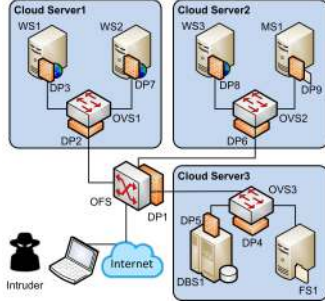


Fig. 4: Virtual network topology used in the validation

5.7 Discard Useless Optimal CMs

Now, for each attack path we have selected an optimal countermeasure to secure that path. We may have useless countermeasures such that their effect can be covered by others either on the same defense point or different ones. In the case more than one countermeasure is selected on the same defense point; we select the strongest one according to a pre-ordered countermeasure list. For instance, shutting down a service is stronger than restarting that service. For the second case, let us have two attack paths comprising these defense points sequences: $\{dp_1, dp_3\}$ and $\{dp_1, dp_2, dp_3\}$. Imagine that the target service is protected by dp_3 . Assume that the optimal countermeasure for the first attack path is shutting down service s_x , protected by dp_1 , and the optimal countermeasure for the second attack path is restarting the target service. As can be seen, the second one is useless if we shut down the service s_x . To do so, for two countermeasures each of whose related defense points are located in the same path, we keep the first visited one in the path if it is stronger than the second one; otherwise, we keep both. After discarding the useless optimal countermeasures, the remaining ones are deployed on related defense points.

6 EXPERIMENTAL RESULTS

6.1 Simulation Setup and Integration in Cloud

To show the feasibility of our approach and test it in a real cloud, we integrated our framework in Openstack. To do so, a Cloud Intrusion Countermeasure Selection (CICS) was designed to interact with openstack control services. To realize the service chaining and traffic steering in Openstack, we used OpenDaylight. To validate the proposed framework, we use a cloud network topology consisting of three servers connected to the Internet through a physical openFlow-capable switch, as seen in Figure 4. The first cloud server hosts two VMs, used as two web servers ($WS1 : HR$ and $WS2 : Portal$), that are connected to a virtual switch ($OVS1$). The second cloud server hosts two VMs, the first one hosts a web server ($WS3 : Finance$); the second one hosts a mail server ($MS1 : Mail$). Similarly, these VMs are connected to a virtual switch $OVS2$. The third cloud server hosts two VMs, used as a database server ($DBS1 : DB$) and a file server ($FS1 : File$) that are connected to a virtual switch $OVS3$. Each VM possesses a set of vulnerabilities, represented in Table 1.

6.2 Attack Scenario

Figure 5 shows the ADT for our virtual network topology. As seen, there are many attack paths to compromise the database system. We programmed the Snort IDS to generate alerts with

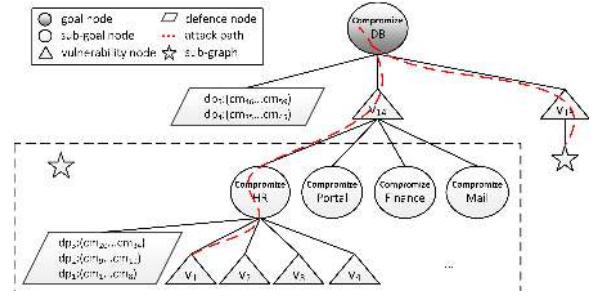


Fig. 5: Attack Scenario in Attack-Defense Tree.

TABLE 1: VMs and their vulnerabilities

Server	VM	CVE	Vulnerability
Cloud Server 1	WS1 (Apache)	v_1 : CVE-2007-1741	Execute code gain privileges
		v_2 : CVE-2014-6271	Remote code execution
		v_3 : CVE-2012-4558	XSS vulnerability
		v_4 : CVE-2014-0098	DoS
	WS2 (IIS)	v_5 : CVE-2009-1535	WebDAV Authentication Bypass
		v_6 : CVE-2009-3023	Memory Corruption
Cloud Server 2	WS3 (Apache)	v_7 : CVE-2014-6271	Remote code execution
		v_8 : CVE-2012-0883	Gain privilege
		v_9 : CVE-2014-0098	DoS
	MS1	v_{10} : CVE-2004-0840	Remote code execution
		v_{11} : CVE-2001-1030	Squid port scan
Cloud Server 3	FS1	v_{12} : CVE-2007-5616	Buffer overflow
		v_{13} : CVE-2001-0755	Buffer overflow
	DBS1	v_{14} : CVE-2008-5416	DoS
		v_{15} : CVE-2008-0107	Memory Corruption

CVE id. Then, the CICS framework can map the CVE alert to the ADT. The attacker in the first step exploits the vulnerability v_1 , CVE-2007-1741, in Apache 2.2.3, which is running on WS1. After exploiting the first vulnerability, the attacker uses the connection to the Database Server to compromise it. When the vulnerability v_1 is compromised, two attack paths are identified to compromise the goal node. As explained in Section 5.4, we eliminate one of the attack paths, since they visit the same sequence of defense points. As Figure 5 shows, there are five defense points in the attack path to stop the attacker. Table 2 gives a list of possible countermeasures at the five defense points. In the next subsections, we show the results of the security performance, security impact on QoS, and security cost evaluations for each candidate countermeasure. Finally, the optimal countermeasure is selected by evaluating the Pareto optimal set with respect to the attack damage cost.

6.3 Security Performance Evaluation

Figures 6a and 6b represent the history of successes and failures of all the countermeasures over time. To be fair, we wanted to have a large history for each countermeasure. During six months, we generated 5,691 attacks to compromise 15 vulnerabilities presented in the ADT. Each time, our IRS selected a countermeasure, deployed it, evaluated its success, and stored the result in the database. The efficiency time (Δt) for evaluating the success and failure of a countermeasure is equal to 5 seconds. If we show the results for the first attack, without history, all the countermeasures have the same goodness, which is not a case in practice.

Based on our ADT model, each type of countermeasure can be applied on different defense points to stop an attack. We never use the same history of goodness for the same type of countermeasure on different defense points. For example, countermeasures cm_1 , cm_9 , and cm_{20} are of a kind that blocks attacker IP, but they have different success and failure rates. 84 successes on defense point dp_1 means that the attacker did not change his IP address and he did not try or did not know the different paths to the root of tree. In contrast, 46 failures on defense point dp_1 refer to the fact that either the attacker changed his IP address and

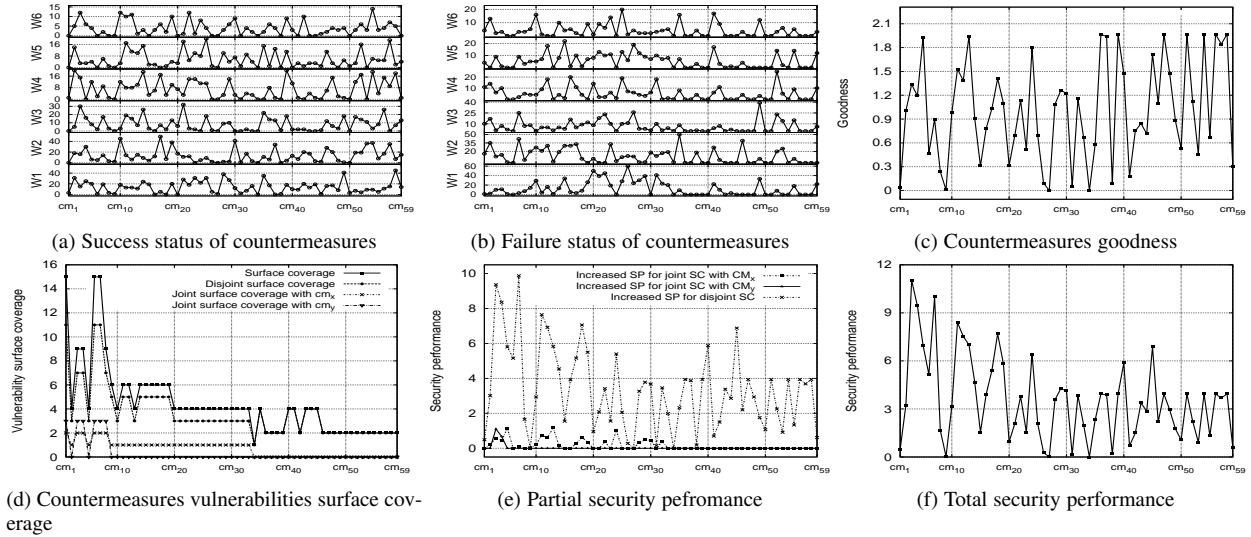


Fig. 6: The result of security performance (S_P), the first objective.

TABLE 2: Possible countermeasures on each defense point.

dp_1	Countermeasure	dp_2	Countermeasure	dp_3	Countermeasure	dp_4	Countermeasure	dp_5	Countermeasure
cm_1	BlockIP(FW,s,attacker)	cm_9	BlockIP(vFW,s,attacker)	cm_{20}	BlockIP(vFW,s,attacker)	cm_{35}	BlockIP(vFW,s,WS1)	cm_{46}	BlockIP(vFW,s,WS1)
cm_2	BlockIP(FW,r,WS1)	cm_{10}	BlockIP(vFW,r,WS1)	cm_{21}	BlockIP(vFW,r,WS1)	cm_{36}	BlockIP(vFW,r,DBS1)	cm_{47}	BlockIP(vFW,r,DBS1)
cm_3	BlockPort(FW,r,http)	cm_{11}	BlockPort(vFW,r,http)	cm_{22}	BlockPort(vFW,r,http)	cm_{37}	BlockPort(vFW,r,mysql)	cm_{48}	BlockPort(vFW,r,mysql)
cm_4	BlockIPPort(FW,s,attacker,http)	cm_{12}	BlockIPPort(vFW,s,attacker,http)	cm_{23}	BlockIPPort(vFW,s,attacker,http)	cm_{38}	BlockIPPort(vFW,s,WS1,http)	cm_{49}	BlockIPPort(vFW,s,WS1,http)
cm_5	BlockIPPort(FW,WS1,http)	cm_{13}	BlockIPPort(vFW,WS1,http)	cm_{24}	BlockIPPort(vFW,WS1,http)	cm_{39}	BlockIPPort(vFW,DBS1,mysql)	cm_{50}	BlockIPPort(vFW,DBS1,mysql)
cm_6	BlockAllTraffic(FW)	cm_{14}	BlockAllTraffic(vFW)	cm_{25}	BlockAllTraffic(vFW)	cm_{40}	BlockAllTraffic(vFW)	cm_{51}	BlockAllTraffic(vFW)
cm_7	Restart(FW)	cm_{15}	Restart(vFW)	cm_{26}	Restart(vFW)	cm_{41}	Restart(vFW)	cm_{52}	Restart(vFW)
cm_8	CloseConnection(http)	cm_{16}	CloseConnection(http)	cm_{27}	CloseConnection(http)	cm_{42}	CloseConnection(mysql)	cm_{53}	CloseConnection(mysql)
		cm_{17}	Disconnect(CloudServer1)	cm_{28}	Disconnect(WS1)	cm_{43}	Disconnect(CloudServer3)	cm_{54}	Disconnect(DBS1)
		cm_{18}	Restart(CloudServer1)	cm_{29}	Restart(WS1)	cm_{44}	Restart(CloudServer3)	cm_{55}	Restart(DBS1)
		cm_{19}	Shutdown(CloudServer1)	cm_{30}	Shutdown(WS1)	cm_{45}	Shutdown(VS3)	cm_{56}	Shutdown(DBS1)
				cm_{31}	Kill(http(HR))			cm_{57}	Kill(mysql)
				cm_{32}	Disable(http(HR))			cm_{58}	Disable(mysql)
				cm_{33}	Restart(http(HR))			cm_{59}	Restart(mysql)
				cm_{34}	Patch(http(HR),CVE-2007-1741)				

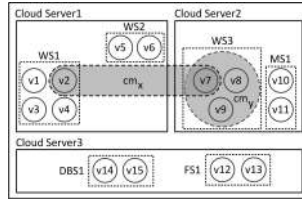


Fig. 7: The status of covering vulnerabilities when two applied countermeasures are still active. cm_x is filtering shellshock attack in HTTP request on defense point dp_1 and cm_y is blocking http request on defense point dp_6 .

launched the attack in the previous attack path or he has a good knowledge of other possible paths to compromise the target. We observe that the highest execution ($success + failure$) belongs to $cm_{25} = BlockAllTraffic(vFW)$ on dp_3 . In contrast, the lowest execution belongs to $cm_{34} = Patch(httpd(HR), CVE - 2007 - 1741)$ on the same defense point.

Fourteen countermeasures, belong to dp_4 and dp_5 , have zero failure. This means that when a countermeasure blocks, isolates, or disables the database system, there is no way to compromise it. Figure 6c shows the result of countermeasure goodness, which is based on the formula presented in (20). The goodness of 50% of the countermeasures is above 1, which indicates that the number of successes was greater than the number of failures in all windows.

Figure 7 illustrates the status of VSC model when two deployed countermeasures, cm_x and cm_y , are still active. cm_x has been deployed before cm_y with the goal of filtering the shellshock attack in HTTP request by adding some WAF (web application firewall) rules on dp_1 . These WAF rules cover two vulnerabilities

in two services: the portal and finance web applications on cloud servers 1 and 2, respectively. Countermeasure cm_y has been applied on dp_6 (vFW in cloud server 2), to block an attempt to compromise the finance web application through exploiting vulnerability v_8 . Since the goodness of cm_y (0.969) is greater than that of cm_x (0.774), v_7 is considered protected by cm_y .

As seen in Figure 5, five defense points exist in the attack path. All possible countermeasures presented in Table 2 are inserted individually in our framework, which takes into account all already deployed active countermeasures (as shown in Figure 7). A countermeasure vulnerabilities surface coverage may have joint surfaces with the two already deployed active countermeasures: cm_x and cm_y . For example, when $cm_3 = BlockPort(FW, r, http)$ is applied on dp_1 the total vulnerabilities surface coverage is 15. The joint surface of cm_3 with cm_x (filtering shellshock) consists of two vulnerabilities (v_2 and v_7) and with cm_y consists of three vulnerabilities (v_7 , v_8 , and v_9). When the blocking port countermeasure is applied on another defense point, its surface coverage and joint surface change. For example, if we apply $cm_{11} = BlockPort(vFW, r, http)$ on dp_2 the total vulnerabilities surface coverage is 6 and has 1 (v_2) and 0 vulnerability in the joint surface coverage with cm_x and cm_y , respectively.

Figure 6d shows the number of vulnerabilities surface coverage in disjoint and joint surfaces with countermeasures cm_x and cm_y . As can be seen, the countermeasures on defense point dp_1 have the larger joint surface with cm_x and cm_y , while the countermeasures on defense point dp_4 and dp_5 do not have any joint surface with the currently deployed active countermeasures. Figure 6e shows the partial surface coverage for each countermeasure when it is applied in the framework. The security performance

for disjoint surface is the number of covered vulnerabilities times the countermeasure goodness, see (23). In contrast, the security performance for joint surface with already deployed active countermeasures depends on their goodness. If a new countermeasure has less goodness compared to the one that has joint surface with it, it cannot increase the security performance and this surface is ignored, see (24). Thus, if a countermeasure has small disjoint surface coverage and small goodness, it cannot increase the total security performance. Consequently, it has little chance of being selected unless it occupies a big role in the other two objectives. Figure 6f represents the final result of the first objective for 59 countermeasures. We observe that cm_3 , which is blocking an http request on dp_1 , has the best S_P . In contrast, cm_{34} , which is patching the vulnerability, has the worst S_P , while the security performance of cm_9 and cm_{27} are very close to zero.

6.4 Security Impact on Service Quality Evaluation

In this subsection, we evaluate the results of our second objective, which is the negative impact of countermeasures on service quality. Figure 8a illustrates the power of each countermeasure, which represents its ability to deal with an attacker, and it is bounded between 1 and 3. As can be seen in Figure 8a, blocking sender/receiver ip/port (e.g., cm_3) are strong countermeasures while restarting VM or FW/vFW (e.g., cm_7) are weak countermeasures to stop the progress of an attacker. As explained in subsection 5.5.2, to evaluate the negative impact of a countermeasure, two types of impacts are considered: *direct* and *backward*. Figure 10 shows the service dependency graph setup in the defined virtual network topology and the severity of dependency between services in terms of CIA. Because of the lack of such data in the literature, we have set reasonable values, as presented in the figure.

To calculate any type of impact, we need to know the number of online users for each service. The number of online users at attack time for HR, Portal, Finance, Mail, FTP, and DB are 20, 50, 0, 300, 1, and 1, respectively. Since the finance web application has been blocked by countermeasure cm_y , no user can connect to this service. Since DB and FTP services cannot be accessed by public users, one user who is the administrator is considered for them. Based on (26), α and β (which express the relative importance between users and services) are initialized to 0.4 and 0.6. Figure 8b shows the result of direct and backward impact evaluation.

As can be seen in Figure 8b, the highest direct impact belongs to countermeasures cm_6 and cm_7 that blocks all traffic and restarts the firewall, and so no online users can connect to the services. Countermeasures cm_1 to cm_{34} , which are deployed on defense points dp_1 , dp_2 , or dp_3 , do not have any backward impact. In contrast, countermeasures cm_{35} to cm_{59} , which are deployed on either defense point dp_4 or dp_5 , have backward impact on DB.

Figure 8c shows the result of the second objective function, which is evaluating the countermeasures' impact on QoS. As can be seen, the highest impact is related to cm_6 , which blocks all traffic on dp_1 . This countermeasure blocks all online users and has a big impact on QoS. In the second place, we see countermeasures $cm_{40} = BlockAllTraffic(vFW)$, $cm_{43} = Disconnect(CloudServer3)$, and $cm_{45} = Shutdown(CloudServer3)$ on dp_4 . Each of these countermeasures disconnects the relationship between services and DB service. In contrast, four countermeasures have the lowest impact on QoS (2.62): cm_1 , cm_9 , cm_{20} , and cm_{23} . They block attacker IP on dp_1 , dp_2 , and dp_3 or block attacker IP-httpport on dp_3 . The impact of these types of countermeasures is

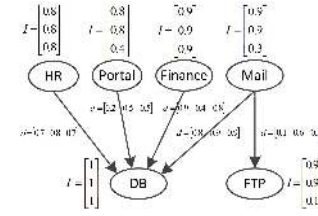


Fig. 10: Service dependency graph of the proposed topology.
TABLE 3: Pareto optimal solutions

defense point	CMs	Description	S_P	S_Q	S_C
dp_1	cm_3	BlockPort(FW,r,http)	11.03	16.98	2.00
	cm_4	BlockIPPort(FW,s,attacker,http)	9.44	4.35	2.00
	cm_7	Restart(FW)	10.00	20.83	1.13
dp_2	cm_{11}	BlockPort(vFW,r,http)	8.40	16.98	1.34
	cm_{12}	BlockIPPort(vFW,s,attacker,http)	7.53	4.35	1.34
	cm_{16}	CloseConnection(http)	3.93	5.66	1.00
	cm_{18}	Restart(CloudServer1)	7.69	11.32	1.23
dp_3	cm_{23}	BlockIPPort(vFW,s,attacker,http)	1.56	2.62	1.10
	cm_{24}	BlockIPPort(vFW,WS1,http)	6.42	8.70	1.10
	cm_{27}	CloseConnection(http)	0.004	2.90	1.00
	cm_{29}	Restart(WS1)	4.27	5.80	1.23
dp_5	cm_{47}	BlockIP(vFW,r,DBS1)	3.94	26.06	1.05

on one user (the attacker), and does not have any impact on other users. The next impact at the next level (2.9) belongs to $cm_{27} = CloseConnection(http)$ on defense point dp_3 , which is a WAF firewall close to HR machine and has merely a transient impact only on HR online users.

6.5 Security Deployment Cost Evaluation

Figure 9 shows the results of security deployment cost, which is based on incompatibility and administration costs. We define the countermeasure incompatibility cost through the number of rules in each firewall, which are 150, 85, 55, 75, and 45 on dp_1 , dp_2 , dp_3 , dp_4 , and dp_5 , respectively. The boundaries of the Smf function in (29) are $a = 20$ and $b = 200$. These boundaries are defined for the worst case scenario when the new rule has to be compared with the entire set of rules [18]. As can be seen in Figure 9a, since there are more rules in the first firewall on dp_1 , there is more incompatibility cost for cm_1 to cm_8 .

Figure 9b illustrates the administration cost when a countermeasure is deployed. As revealed, the insertion of all firewall rules does not have any administration cost (equal to 1). The highest value belongs to patching a vulnerability, which is equal to 3. After that, the highest value is related to shutting down or restarting a server or virtual machine on which an administrator needs to do some operations to return the system to its previous configuration.

Figure 9c illustrates the final result for the third objective function. Based on (28), γ and δ , which express the relative importance between the incompatibility and administration costs, are initialized to 0.7 and 0.3, respectively. If the system administrator does not have time to do the configuration after each deployment, he can set it to 0.9 and 0.1. In contrast, when the number of rules increases, the performance of the firewall degrades. In this case, γ and δ can be set to 0.1 and 0.9, respectively. As shown in Figure 9c, inserting firewall rules on defense point dp_1 results in the highest security cost compared to other countermeasures.

6.6 Optimal Countermeasure Selection

Now, let us solve (1) to evaluate the different trade-offs between S_P , S_Q , and S_C and identify the set of best solutions as well as the optimal one. The obtained results are presented in Figure 11, which shows all the solutions and the Pareto optimal set. Each defense point's countermeasures are shown with

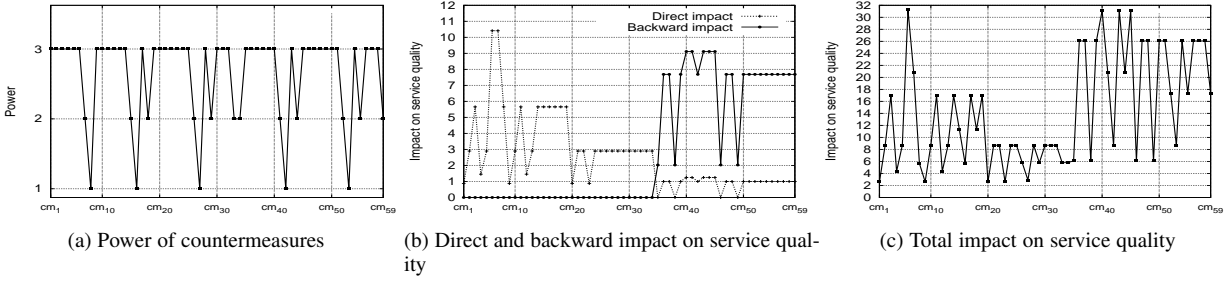


Fig. 8: The evaluation of countermeasure negative impact on service quality (S_Q), the second objective.

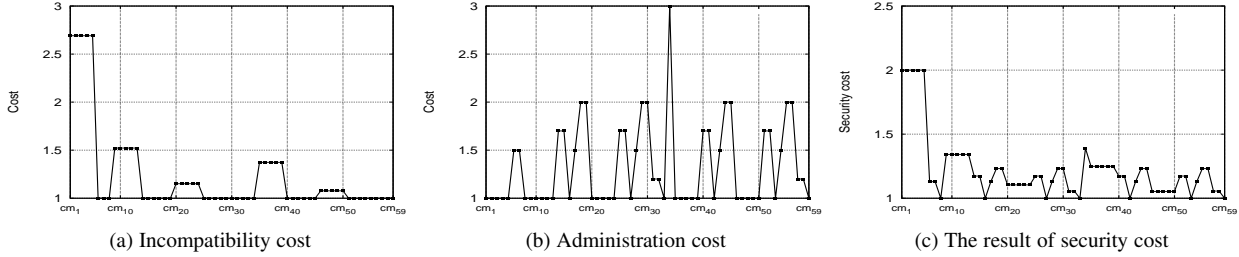


Fig. 9: The result of security cost (S_C), the third objective.

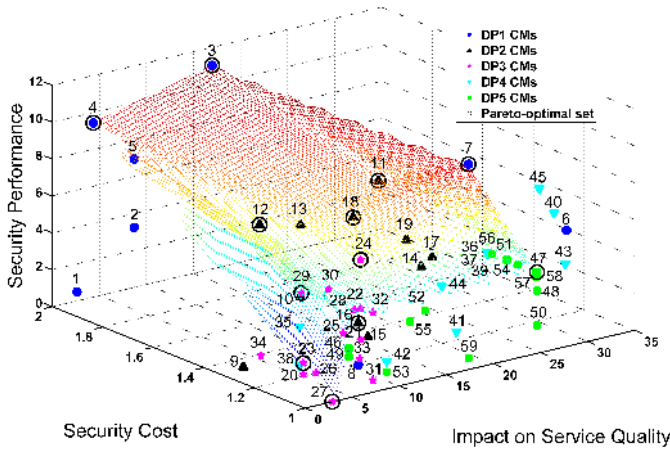


Fig. 11: The results of our multi-objective optimization-based framework. Represented are the optimal (inside black circles) and non-optimal solutions.

different colors and shapes. The optimal solutions in Figure 11 are summarized in Table 3. The returned optimal countermeasures (those lying on the Pareto optimal surface) belong to all defense points except dp_4 . If we focus on security performance, $cm_3 = BlockPort(FW, r, http)$ represents the best countermeasure with the highest S_P value (11.03). However, it generates a high impact on service quality ($S_Q = 16.98$). The worst in security performance from the Pareto optimal set is $cm_{27} = CloseConnection(http)$, which has lower vulnerabilities surface coverage (see Figure 6d) and goodness (close to zero, see Figure 6c). However, it provides less impact on service quality (2.90) since it closes only the HR application users' connections.

We observe that some countermeasures are selected from different defense points because they yield different trade-offs between the objective functions: 1) $BlockPort(FW(or vFW), r, http)$, 2) $CloseConnection(http)$, and 3) $BlockIPPort(FW(or vFW), s, attacker, http)$. For instance, blocking the attacker's IP and http port has been selected on three defense points with different security performance (9.44, 7.53, and 1.56),

security impact (4.35, 4.35, and 2.62), and security cost (2.00, 1.34, and 1.10). If we ignore dimension S_C , cm_{12} should likewise be ignored because of less security performance compared to cm_4 .

Furthermore, as shown in Figure 11, the majority of countermeasures on dp_4 and dp_5 (except cm_{47}) are dominated (in the sense of multi-objective optimization) and far from the Pareto optimal surface. Since these countermeasures, which are applied on cloud server 3, are close to the target ($DBS1$), they provide less vulnerabilities surface coverage, and thus less S_P . Besides, they have a high direct impact on $DBS1$ and backward impact on four services that have direct dependency on $DBS1$ (see Figure 10). That is why these countermeasures are not selected and are far from the Pareto optimal surface (low S_P with high S_Q).

Now, we select the optimal solution from the Pareto optimal set using SAW method, with respect to the attack damage cost. Figure 12 represents the result of the attack damage cost evaluation when vulnerability CVE-2007-1741 is exploited in service HR. As explained, the damage cost consists of current and potential damages which are 2.4 and 7.45 in terms of CIA, respectively. So, the total damage cost is 9.85. Since, no service uses HR, the current backward damage from HR is zero, while the backward damage from DB is high. As shown in Figure 12, the total value of services in our framework is 14.1, in terms of CIA. Therefore, the total damage cost for the whole system from the exploited vulnerability is 69%. For this attack damage cost value, cm_3 is selected as the optimal one.

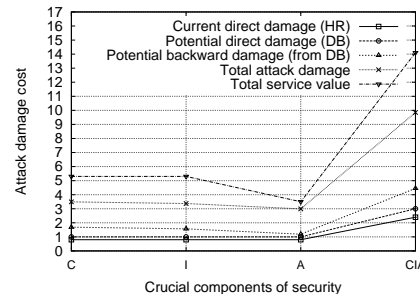


Fig. 12: Attack damage cost in terms of CIA.

TABLE 4: The first three optimal countermeasures selected by SAW, PW, and TOPSIS with respect to attack damage cost variation (w_P). Based on (9), the other two weights, w_Q and w_C , are obtained using w_P and $\sigma = 0.6$ and $\theta = 0.4$.

		w_P				
		0.1	0.3	0.5	0.7	0.9
SAW	1 st optimal cm	cm_{23}	cm_{23}	cm_4	cm_3	cm_3
	2 nd optimal cm	cm_{27}	cm_{12}	cm_{12}	cm_4	cm_7
	3 rd optimal cm	cm_{12}	cm_{27}	cm_7	cm_7	cm_4
PW	1 st optimal cm	cm_{23}	cm_{12}	cm_4	cm_4	cm_3
	2 nd optimal cm	cm_{12}	cm_4	cm_{12}	cm_{12}	cm_4
	3 rd optimal cm	cm_{16}	cm_{23}	cm_{24}	cm_3	cm_7
TOPSIS	1 st optimal cm	cm_{12}	cm_{18}	cm_{18}	cm_{47}	cm_{47}
	2 nd optimal cm	cm_4	cm_{24}	cm_{24}	cm_{18}	cm_{18}
	3 rd optimal cm	cm_{24}	cm_{12}	cm_7	cm_7	cm_7

6.6.1 Reliability of the Obtained Optimal Result

In this section, we show that the SAW method used provides reasonable results, compared to other well-known scoring methods: PW and TOPSIS. Besides SAW, we also implemented PW and TOPSIS. Table 4 illustrates the three optimal solutions from the Pareto optimal set resulted by the three methods, when the severity of attack damage cost varies between 0.1 to 0.9. We observe that: (1) when w_p is low, 0.1, SAW and PW select reasonable countermeasures compared to that selected by TOPSIS (cm_{23} vs. cm_{12}). That is, cm_{12} provides higher S_P than cm_{23} , and that incurs higher impact on S_Q , see Table 3. cm_{12} blocks two VMs in cloud server 1, while cm_{23} only blocks one VM (HR). Such high impact on S_Q is not needed as w_p is low, (2) in case of high w_p , 0.9, the countermeasure selected by TOPSIS, cm_{47} , provides low S_P (3.94) compared that selected by SAW and PW, which is cm_3 (11.03). Moreover, cm_{47} incurs higher impact on S_Q (26.06) compared to that selected by SAW and PW (16.98). From the security perspective, cm_{47} provides less protection (only DB in the network), and high impact on service quality (all VMs: HR, Portal, Finance, and Mail, see Figure 10). On the other hand, cm_3 provides higher protection (all http servers), and less impact on service quality compared to cm_{47} (no impact on Mail server), and (3) when w_p is equal to 0.3 and 0.7, SAW performs better than PW. That is, when $w_p = 0.3$, which is somehow low, SAW selected less strong countermeasure than that selected by PW. On the opposite, when $w_p = 0.7$, which is somehow high, SAW selects stronger countermeasure than that selected by PW. On a final note, we conclude that SAW performs better all the time.

Now let us have a deep insight on the optimal countermeasures selected by SAW. If we consider the first optimal solutions for different weight combinations, we can see that when the attack is weak ($w_p < 0.5$), the block attacker IPPort(http) is selected (cm_{23} on dp_3). When the severity of damage is a middle value, the same countermeasure is selected, but on different places with more severe effects (cm_4 on dp_1). It blocks the attacker from accessing any http service. When the severity of the attack is high, cm_3 on dp_1 is selected to block all users' access to any http service. Countermeasures cm_4 , cm_{12} , and cm_{23} are of a kind, but have different effects because of their deployment positions. As can be seen, cm_4 , which is stronger than others, appears when $w_p \geq 0.5$. cm_{27} , which closes the http connections on dp_3 , behaves similarly to cm_{23} .

6.7 Performance Evaluation

In this subsection, we present the asymptotic complexity and real-time performance of the CICS framework. As shown in Table 5, the complexity in the worst case is $\mathcal{O}(|CM|^2 + (|S| + |W| + |V| + |CM_a|) \cdot |CM|)$, where $|CM|$ is the number of possible countermeasures that can be deployed on all defense points, $|S|$ is

TABLE 5: Complexity of the proposed framework

Operation type		Complexity	
		Partial	Total
ADC	Current impact	$\mathcal{O}(S)$	$\mathcal{O}(S)$
	Potential impact	$\mathcal{O}(S)$	
S_P	Goodness	$\mathcal{O}(W)$	$\mathcal{O}(CM \cdot (W + V + CM_a))$
	Surface coverage (SC)	$\mathcal{O}(V)$	
	Joint SC with CM_a	$\mathcal{O}(CM_a)$	
S_Q	Direct impact	$\mathcal{O}(S)$	$\mathcal{O}(CM \cdot S)$
	Backward impact	$\mathcal{O}(S)$	
S_C	Incompatibility Administration	$\mathcal{O}(1)$	$\mathcal{O}(CM)$
		$\mathcal{O}(1)$	
MOPT	Pareto optimal set SAW	$\mathcal{O}(CM ^2)$	$\mathcal{O}(CM ^2)$
Total		$\mathcal{O}(CM ^2 + (S + W + V + CM_a) \cdot CM)$	

the number of services in the SDG, $|W|$ is the number of windows in goodness evaluation, $|V|$ is the number of vulnerabilities, and $|CM_a|$ represents the number of active countermeasures. ADC evaluation depends on the importance of services, severity of dependency between them in terms of CIA, and the number of service vulnerabilities. Since all these parameters are static, the attack damage cost of each vulnerability can be evaluated and stored in the database in advance. Over time, when any change happens to these parameters, the ADC is updated. Note that S_P , S_Q , and S_C are dynamic, but S_P and S_C can be evaluated between two attack times, whereas S_Q should be evaluated at attack time. Let us consider two attack times: t_1 and t_2 ($t_1 < t_2$). When an optimal countermeasure is applied at t_1 , we wait Δt , (which is efficiency time), ($t_1 + \Delta t < t_2$) to monitor the success and failure status of the applied countermeasure and update its S_P . Similarly, S_C is updated only when a new firewall rule is added. (Note that only one type of countermeasure, which is rule insertion, can impact (29).) In contrast, because S_Q depends on the number of online users, it should be updated at attack time. In this case, the complexity of our framework is $\mathcal{O}(|CM|^2 + |S| \cdot |CM|)$.

The performance of our framework has been evaluated only for the response system when the CICS framework receives the alerts from the IDS. We distinguish two times: the time needed to obtain the optimal countermeasure and the time to deploy it. Obtaining the optimal countermeasure, from a list of 59 countermeasures, takes 314ms. The optimal countermeasure to stop our attack scenario is cm_3 , which blocks the http port in the physical firewall on dp_1 . Since this firewall has 150 rules, the insertion incompatibility process takes 135ms. Our framework was prototyped on a machine with 6 cores Intel Westmere (XEON L5638) clocked at 2.30 GHz with 24 GB RAM. In total, the CICS framework takes about 449ms for our attack scenario. It is reasonably fast in deciding which countermeasure is the optimal one.

7 CONCLUSION

In this paper a dynamic framework for selecting and deploying an optimal countermeasure to mitigate attack in an online fashion was proposed. The advantage of the proposed framework is that the selected countermeasure can be fine-tuned on the basis of the context in which the attack is detected. In other words, the selection mechanism takes into account the trade-off between maximizing the security benefit, minimizing the security impact on users and services, and minimizing the security deployment cost. Thus, the countermeasures are not predictable since they are not statically determined. This reduces the possibility of attackers exploiting the predictability and the potential security impact caused by unnecessary countermeasures. Compared to existing work, all the proposed objective functions are dynamic, which reflect the dynamicy of the network status (appearing or

disappearing users, services, and vulnerabilities), the complexity of security appliances, and the goodness of countermeasures over time. Experimental results show the applicability and performance of the proposed framework in, but not limited to, the cloud.

For future work, it would be worthwhile to investigate supporting multiple ADTs at the same time. As explained in Section 5, different ADTs can be defined based on the SDG in such a way that each ADT protects one goal service. Our framework was designed for one ADT at the time.

ACKNOWLEDGMENT

This work is partly funded by Natural Sciences and Engineering Research Council of Canada Research Chair on Sustainable Smart Eco-Cloud, NSERC-950-229052 and by the NSERCCRDJP 424371-11: ECOLOTIC Sustainable and Green Telco-Cloud.

REFERENCES

- [1] A. Shameli-Sendi, M. Cheriet, and A. Hamou-Lhadj, "Taxonomy of intrusion risk assessment and response system," *Computers & Security*, vol. 45, pp. 1-16, 2014.
- [2] H. Wei, D. Frinke, O. Carter, and C. Ritter, "Cost-benefit analysis for network intrusion detection systems," *CSI 28th Annual Computer Security Conference*, Washington, DC, 2001.
- [3] N. McKeown, T. Anderson, H. Balakrishnan, G. Parulkar, L. Peterson, J. Rexford, S. Shenker, and J. Turner, "OpenFlow: enabling innovation in campus networks," *ACM SIGCOMM Computer Communication Review*, vol. 38, no. 2, pp. 69-74, 2008.
- [4] N. Kheir, N. Cuppens-Bouahia, F. Cuppens, and H. Debar, "A service dependency model for cost sensitive intrusion response," *Proceedings of the 15th European Conference on Research in Computer Security*, pp. 626-642, 2010.
- [5] N. Kheir, H. Debar, N. Cuppens-Bouahia, F. Cuppens, and J. Viinikka, "Cost evaluation for intrusion response using dependency graphs," In *IFIP International Conference on Network and Service Security*, 2009.
- [6] I. Balepin, S. Maltsev, J. Rowe, and K. Levitt "Using specification-based intrusion detection for automated response," *Proceedings of the 6th International Symposium on Recent Advances in Intrusion Detection*, pp. 136-154, 2003.
- [7] S. Zonouz, R. Berthier, H. Khurana, W. Sanders, and T. Yardley, "Seclius: An Information Flow-based, Consequence-centric Security Metric," *IEEE Transactions on Parallel and Distributed Systems*, vol. 26, no. 2, 2013.
- [8] R. Marler and J. Arora, "Survey of multi-objective optimization methods for engineering," *Structural and Multidisciplinary Optimization*, vol. 26, no. 6, pp. 369-395, 2004.
- [9] F. Gembicki and Y. Haimes, "Approach to performance and sensitivity multiobjective optimization: The goal attainment method," *IEEE Transactions on Automatic Control*, vol. 20, no. 6, pp. 769-771, Dec. 1975.
- [10] C.-J. Chung, P. Khatkar, T. Xing, J. Lee, and D. Huang, "NICE: Network intrusion detection and countermeasure selection in virtual network systems," *IEEE Transactions on Dependable and Secure Computing (TDSC)*, vol. 5, no. 4, pp. 198-211, 2013.
- [11] C. Hwang and K. Yoon, "Multiple attribute decision making : Methods and applications," Springer-Verlag, 1981.
- [12] P. Ammann, D. Wijesekera, and S. Kaushik, "Scalable, graph-based network vulnerability analysis," In *Proceedings of the 9th ACM Conference on Computer and Communications Security*, pp. 217-224, 2002.
- [13] S. Jha, O. Sheyner, and J. Wing, "Two formal analyses of attack graphs," In *Proceedings of the 15th Computer Security Foundations Workshop*, pp. 49-63, 2002.
- [14] A. Roy, D. S. Kim, and K. S. Trivedi, "Attack countermeasure trees (ACT): towards unifying the constructs of attack and defense trees," *Security and Communication Networks*, vol. 5, no. 8, pp. 929-943, 2012.
- [15] B. Kordy, S. Mauw, S. Radomirovi, and P. Schweitzer, "Foundations of AttackDefense Tree," In: *FAST. LNCS*. Springer, Heidelberg, 2010.
- [16] R. Dewri, I. Ray, N. Poolsappasit, and D. Whitley, "Optimal security hardening on attack tree models of networks: a cost-benefit analysis," *Int. Journal of Information Security*, vol. 11, no. 3, pp. 167-188, 2012.
- [17] S. Jajodia, S. Noel, and B. OBerry, "Topological analysis of network attack vulnerability," In *Managing Cyber Threats*, pp. 247-266, 2005.
- [18] E. Al-Shaer and H. Hamed, "Modeling and management of firewall policies," *IEEE Transactions on Network and Service Management*, vol. 1, no. 1, pp. 2-10, 2004.
- [19] N. Poolsappasit, R. Dewri, and I. Ray, "Dynamic security risk management using bayesian attack graphs," *IEEE Transactions on Dependable and Secure Computing*, vol. 9, no. 1, pp. 61-74, 2012.
- [20] Z. Zhang, P. H. Ho, and L. He, "Measuring IDS-estimated attack impacts for rational incident response: A decision theoretic approach," *Computers & Security*, vol. 28, no. 7, pp. 605-614, 2009.
- [21] T. Toth and C. Kregel, "Evaluating the impact of automated intrusion response mechanisms," *Proceedings of the 18th Annual Computer Security Applications Conference*, Los Alamitos, USA, 2002.
- [22] G. G. Granadillo, M. Belhaouane, H. Debar, and G. Jacob, "RORI-based countermeasure selection using the OrBAC formalism," *International journal of information security*, vol. 13, no. 1, pp. 63-79, 2014.
- [23] C. Strasburg, N. Stakhanova, S. Basu, and J. S. Wong, "A Framework for Cost Sensitive Assessment of Intrusion Response Selection," *Proceedings of IEEE Comp. Soft. and App. Conf.*, pp. 355-360, 2009.
- [24] S. Wang, Z. Zhang, and Y. Kadobayashi, "Exploring attack graph for cost-benefit security hardening: A probabilistic approach," *Computers & Security*, vol. 32, pp. 158-169, 2013.
- [25] A. Shameli-Sendi and M. Dagenais, "ARITO: Cyber-attack response system using accurate risk impact tolerance," *International Journal of Information Security*, vol. 13, no. 4, pp. 367-390, 2014.
- [26] NIST, "National vulnerability database, NVD," <http://nvd.nist.gov>.



Alireza Shameli-Sendi is currently an Assistant Professor at Shahid Beheshti University. Before joining SBU, he was Postdoctoral Fellow at Ericsson, Canada and Postdoctoral at ETS and McGill universities in collaboration with Ericsson. He received his Ph.D degree in computer engineering from Ecole Polytechnique de Montreal, Canada. He obtained his B.Sc. and M.Sc. from Amirkabir University of Technology. His primary research interests include information security, intrusion response system, and cloud computing. He is a recipient of Postdoctoral Research Fellowship Award and Industrial Postdoctoral Fellowship Award from Canada.



Information security.

Habib Louafi (S'11) holds an Engineering degree in Computer Science from the University of Oran (Algeria), an M.Sc. from the Université du Québec à Montréal (UQAM), and a Ph.D. from École de technologie supérieure (ÉTS is a part of the Université du Québec network). He is currently working as a postdoctoral fellow at Synchromedia Laboratory for multimedia communication in telepresence (ÉTS). His fields of interest include mobile cloud computing, context-aware systems, multi-objective optimization, and



Wenbo He received the PhD degree from University of Illinois at Urbana-Champaign, Champaign, IL, USA, in 2008. She is currently an Associate Professor in Department of Computing and Software at McMaster University. Before that she was an Assistant Professor in School of Computer Science at McGill University from 2011 to 2016, and was an Assistant Professor in Department of Electrical Engineering at University of Nebraska-Lincoln from 2010 to 2011. She was with the Department of Computer Science at University of New Mexico from 2008 to 2010. Her research focuses on Big Data Systems, Cloud Computing, and Privacy-preserving Techniques, etc.



Mohamed Cheriet received his M.Sc. and Ph.D. degrees in Computer Science from the University of Pierre et Marie Curie (Paris VI) in 1985 and 1988 respectively. Dr. Cheriet is expert in cloud computing and network virtualization. In addition, he is an expert in Computational Intelligence, Pattern Recognition, Mathematical Modeling for Image Processing, Cognitive and Machine Learning approaches and Perception. Dr. Cheriet has published more than 350 technical papers in the field. He holds Canada Research Chair Tier 1 on Sustainable Smart Eco-Cloud.